Table 1. Principal ion-molecule reactions in the mechanism for ozone decomposition by ionizing radiation.

$O_3 \rightsquigarrow O_3^+ + e^-$	Ia
$\rightsquigarrow O_3^* \rightarrow O_2 + O$	Ib
$O_2 \rightsquigarrow O_2^+ + e^-$	IIa
$\rightsquigarrow O_2^* \rightarrow O + O$	IIb
$O_2 + e^- + M \rightarrow O_2^- + M$	IIIa
$O_3 + e^- + M \rightarrow O_3^- + M$	IIIb
$O_3 + O_2^- \rightarrow O_2 + O_3^-$	IV
$O_3^- + O_3 \rightarrow O_2 + O_2 + O_2^-$	V
$O_2^- + O_2^+ \rightarrow O_2 + O + O$	VIa
$O_2^+ + O_3^- \rightarrow O_2 + O_2 + O$	VIb

but from the general knowledge of the intensities used in radon experiments in that period, we may estimate a value for $J\,G_{(\mathrm{ions})}$ of $\sim 10^{15}$ ion pairs per cubic centimeter per second. The ion lifetime at this intensity is therefore 10^{-4} second. Combining this value with that of the time for a cycle shows that more than 2000 ozone molecules should be destroyed per ion pair formed. Considering all the uncertainties in the calculations, the agreement with Lewis' value of 4500 is good.

Third, additional evidence for the importance of the ion mechanism is provided by data on the irradiation of liquid oxygen (*6*). Owing to the cage effect, the lifetime of the ions generated in the liquid phase will be much shorter than in the gas phase, and therefore the process should be less effective in decomposing ozone. Also, a small heat of activation will have a strong inhibiting effect at liquid oxygen temperature. Therefore, G-values for ozone formation as large as 15 should be obtained and indeed have been obtained (*6*).

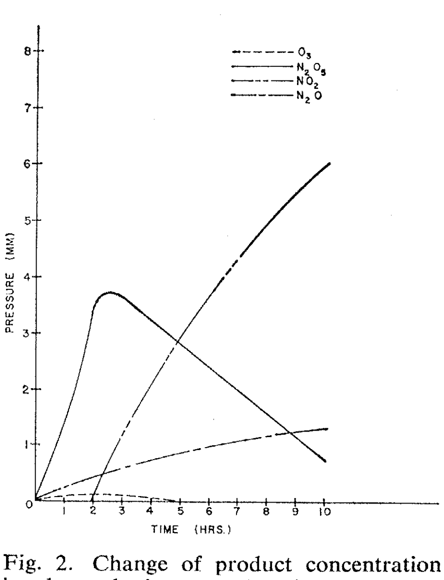

Fig. 2. Change of product concentration in the polonium-210 irradiation of air.

Fourth, there should be methods of breaking the ion-chain mechanism (*7*). One would expect that adding nitrogen dioxide, which has a higher electron affinity than ozone (*5*), to the system would break the negative ion chain by charge transfer:

$$O_3^- + NO_2 \rightarrow O_3 + NO_2^- \qquad \mathrm{VII}$$
$$O_2^- + NO_2 \rightarrow O_2 + NO_2^- \qquad \mathrm{VIII}$$

and result in an increased ozone concentration. Very low concentrations of nitrogen dioxide (parts per million) should be sufficient to break the chain. The results of one group of our continuing series of experiments on the radiolysis of nitrogen-oxygen mixtures show this chain breaking is a possibility. Nitrogen-oxygen mixtures (including air) were irradiated with a Po^{210} alpha source, and the gas mixture was examined continuously during the irradiation with an infrared spectrophotometer. Absorption bands of ozone, nitrogen pentoxide, nitrogen dioxide, and nitrous oxide could be observed, and from their intensities the concentrations of these gases were determined. Most strikingly, in the first 2 hours of irradiation, the ozone concentration was higher by several orders of magnitude than the few parts per million observed in the irradiation of pure oxygen (Figs. 1 and 2). This high concentration of ozone remained even though ozone is consumed to oxidize the nitric oxide and nitrogen dioxide to nitrogen pentoxide, clear evidence thus being provided that the nitrogen oxides do break the ion chain which decomposes ozone.

Unfortunately, as the irradiation proceeds, the simultaneous process of ozone removal by the oxidation of the nitrogen oxides and the thermal decomposition of nitrogen pentoxide result in a net increase in the nitrogen dioxide concentration to the point where the reaction:

$$NO_2 + O \rightarrow NO + O_2 \qquad \mathrm{IX}$$

predominates the formation of ozone:

$$O_2 + O + M \rightarrow O_3 + M \qquad \mathrm{X}$$

Figs. 1 and 2 show the change in the various concentrations with time. The reactions involved have been discussed in detail (*8*).

Thus, even though the nitrogen dioxide can break the negative ion chain that decomposes ozone, the nitrogen dioxide inhibits ozone formation by reacting with oxygen atoms or being oxidized to nitrogen pentoxide. Although interesting from a theoretical viewpoint, the use of nitrogen dioxide is not a means of substantially increasing the ozone concentration.

In conclusion, we have shown that the rate of the decomposition of ozone can be calculated by the ion-chain mechanism of Fueki and Magee. We have also shown that the ion-chain mechanism can be broken by adding a substance with a very high electron affinity. Our initial choice of nitrogen dioxide, while meeting these conditions, was not ideal, because nitrogen dioxide reacts with ozone and oxygen atoms. Therefore, any economical production of ozone from oxygen with strong ionizing radiation sources must involve methods of breaking the ion chain while avoiding other complicating reactions.

P. HARTECK
S. DONDES
B. THOMPSON

Chemistry Department, Rensselaer Polytechnic Institute, Troy, New York

References and Notes

1. K. Fueki and J. L. Magee, *Discussions Faraday Soc.* **36**, 19 (1963).
2. ———, *J. Phys. Chem.* **68**, 2901 (1964).
3. B. J. Lewis, *Phys. Chem.* **37**, 533 (1933).
4. J. F. Kircher, J. S. McNulty, J. L. McFarling, A. Levy, *Radiation Res.* **13**, 452 (1960).
5. M. A. Biondi, *Advan. Electron. Electron Phys.* **18**, 67 (1963).
6. S. Ya. Pshezhetskii, I. A. Myasnikov, N. A. Buneev, *Symposium on Radiation Chemistry* (Acad. of Sciences of the U.S.S.R., Moscow, 1955), p. 133.
7. It would be most advantageous if the ozone decomposition proceeded via negative ions only, as concluded by Fueki and Magee. Because of the large uncertainties in the values reported for the ionization potential of ozone, it may be possible that ozone has a lower ionization potential than oxygen and therefore a positive ion chain cannot be excluded.
8. P. Harteck and S. Dondes, *J. Chem. Phys.* **28**, 975 (1958); USAEC document NYO 9967 (1961).

20 November 1964

Cosmic X-ray Sources

Abstract. *Eight new sources of cosmic x-rays were detected by two Aerobee surveys in 1964. One source, from Sagittarius, is close to the galactic center, and the other, from Ophiuchus, may coincide with Kepler's 1604 supernova. All the x-ray sources are fairly close to the galactic plane.*

Reports of the detection of cosmic x-ray sources with rocket-borne instrumentation have been published (*1–3*). Giacconi, Gursky, Paolini, and Rossi (*1*) obtained the first positive evidence of cosmic x-rays in June 1962. Their instrumentation was designed to survey a broad field of view, and the source of emission was identified with the general vicinity of the center of the galaxy. Bowyer, Byram, Chubb, and Friedman (*2*) attempted a more detailed survey in April 1963, restricting the detector field of view to about 10 degrees. A strong source was observed at right ascension (R.A.), $16^h\ 15^m$, declination $-15°$, in Scorpius, and a weaker source in the Crab Nebula. At the time of flight, the galactic center region was below the horizon. Continuing the search for discrete x-ray sources, we have conducted two additional Aerobee surveys in 1964 from the White Sands Missile Range in New Mexico. The first of these was launched on 16 June when the zenith coordinates were $19^h\ 30^m$ R.A., declination 32.4°. The galactic plane was mapped from the southern region of Scorpius (Sco), through Cygnus (Cyg), to the northern part of Perseus. For the second flight, on 25 November, the zenith R.A. was $8^h\ 48^m$, and the survey extended through Taurus (Tau) to the southern portion of Puppis. We now report the major features that appear in these 1964 surveys.

The mapping technique used in the two 1964 surveys was similar to that used in April 1963. Geiger counters were mounted facing outward through the skin of an unguided Aerobee rocket. Above the atmosphere the rocket executes the motion of a rigid body, characterized by a nearly constant roll rate and a steady precession about a large cone angle. The view at any instant is restricted to a small portion of the sky by means of an aluminum honeycomb collimator which limits the field of view to 8.4° at half maximum transmission. As the rocket rolls and precesses, the view direction sweeps the sky in closely spaced scans. Auxiliary sensors—magnetometers, horizon detectors, and optical star sensors—provide the data from which the history of the view direction is determined for the entire flight.

The Geiger counters were sensitive to wavelengths from 1 to 15 Å. Each counter was constructed in the form of a shallow rectangular box to provide a maximum ratio of window area to volume. Anode wires were strung in parallel and spaced to provide uniform sensitivity over the full volume. The window material was Mylar polyester film spread over the face (553 cm^2) of the counter box. Some of the counters were equipped with ¼-mil Mylar windows and some with ½-mil Mylar windows. With the honeycomb collimator in place, the effective window aperture of each counter was 453 cm^2. By pairing two counters, mounted in the same plane parallel to the length of the rocket, an effective area for x-ray detection of about 906 cm^2 was obtained. This was about 14 times as great as the window area used in the 1963 survey. Two sets of paired counters were used in each rocket and were oriented 180° apart. Because of the large area of plastic film window, a gas flow system was required. The mixture of neon (89 percent), helium (10 percent), and isobutane (1 percent) was maintained at atmospheric pressure.

The counting rates of the individual counters, as well as the summed pairs, were metered by separate rate-meter circuits. In the November flight, the cosmic ray background of one pair of counters was reduced by an anticoincidence arrangement which utilized a third pair of tray counters, with thick windows, mounted back-to-back with the x-ray survey counters.

On 16 June, the rocket reached a peak altitude of 127 km and rolled with a period of about 8.5 seconds. Its precession period was 422 seconds and the precession cone angle was 144°. A solution of the orientation history was obtained to an estimated accuracy of 1.5°. The 25 November flight reached an altitude of 200 km. The roll period was 6.35 seconds, precession period 236 seconds, and cone angle about 140°.

In the June 1964 survey, satisfactory data were obtained from only one pair of counters, which swept across most of the accessible sky. Much of the survey

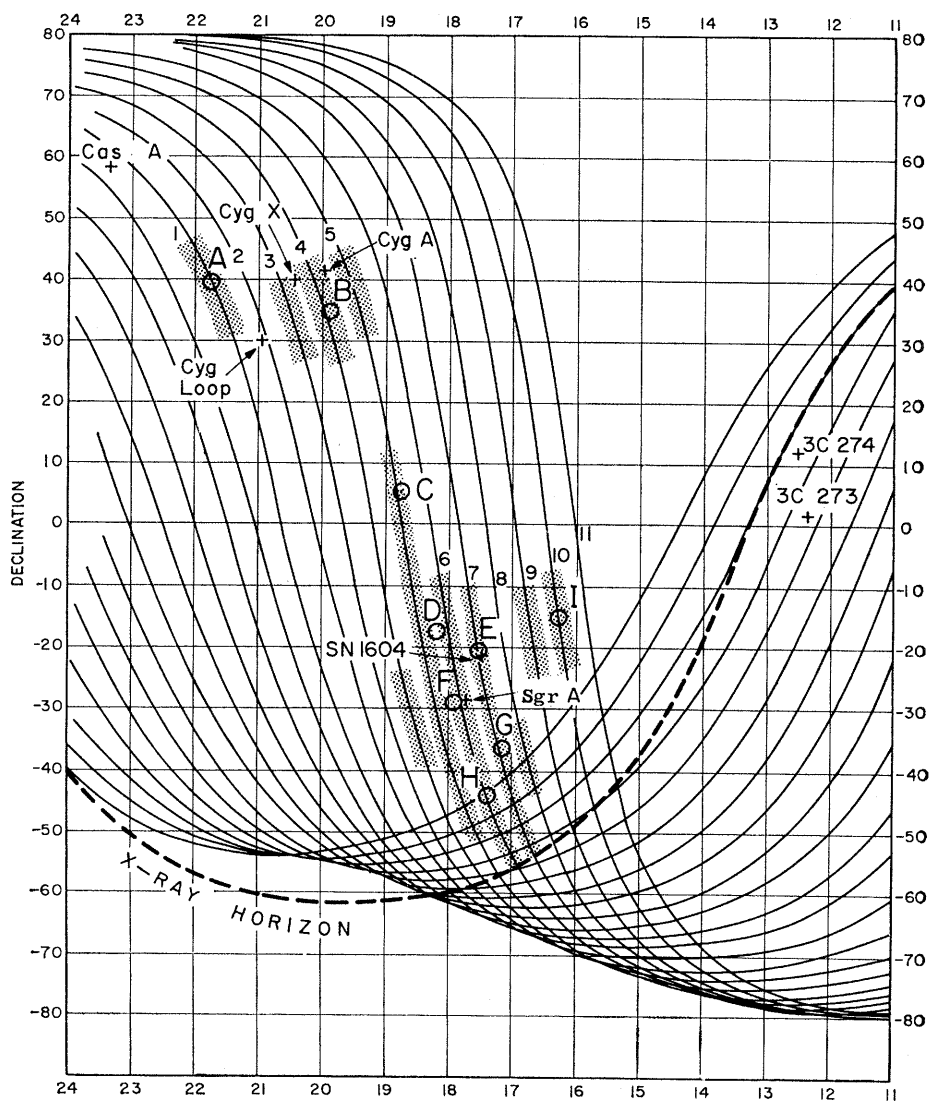

Fig. 1. Map of sky scanned by x-ray detectors in Aerobee flight 16 June 1964. Thin lines trace path of view vector across celestial sphere on successive rolls. Shaded segments indicate portions of scan in which clearly detectable x-ray signals were observed above background. Circles are positions at which discrete sources have been identified.

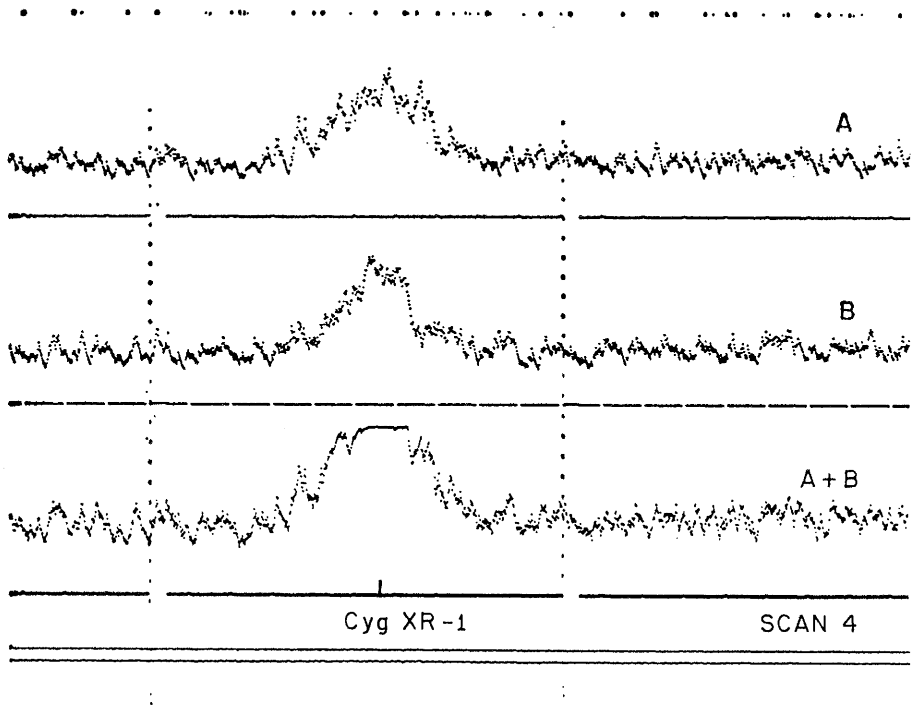

Fig. 2. Telemetry traces of Cyg XR-1 signals. Traces *A* and *B* are from individual counters, each equipped with ¼-mil Mylar window. Trace *A* + *B* is sum of signals from *A* and *B*. Dotted vertical lines are spaced one second apart. Full deflection corresponds to 2000 count/sec.

showed only a statistically varying cosmic ray background with little difference between signals observed above and below. Superposed on this background were several x-ray signal peaks. The thin lines that lace the map of Fig. 1 are the traces of the counter view vector as it swept across the celestial sphere. Where the counters responded above background, the scan lines of Fig. 1 are covered by shaded strips. All of the observed x-ray sources are located relatively near the galactic plane. Those on scans 3, 4, 5, 6, and 7 are within 5° of the galactic equator, and those on scans 1 and 10 are at galactic latitudes of 11° and 22°, respectively.

The isolated responses on scans 9 and 10 fit the position of the Scorpius source, which we derived from the 1963 observation. It remains the strongest source thus far observed. The telemetry record of scan 4 through Cygnus, which shows the second strongest source, is reproduced in Fig. 2.

The strong Scorpius source was observed late in the flight on passes 9 and 10 when the rocket was re-entering the absorbing atmosphere at 100.0 km and 93.4 km. On pass 11, when the rocket was at 86.7 km, no signal was detected. These three observations permit us to deduce roughly the spectral composition and the total flux out to about 10 Å. The pass at 93.4 km scanned directly across the previously determined position of the source. On the preceding and following passes, the displacement of the source relative to the center of the field of view was about 6.5°, so that the collimator transmission was about 25 percent. The filtering effect of the air above the rocket permits us to infer qualitatively the spectral composition. At 93.4 km, with the Scorpius source at an elevation of 22.5°, unit optical thickness of the overhead air mass corresponded to λ (wavelength) equal to 6 Å. The observed flux of 6.6 count cm^{-2} sec^{-1} was, therefore, confined largely to the range 1 to 6 Å. Comparison with the 1963 measurement (*2*) in the 1- to 8-Å range shows a satisfactory agreement. On the preceding pass at 100 km, the counting rate was 4.6 count cm^{-2} sec^{-1}. When corrected for the collimator transmission factor of 25 percent, the flux becomes 18.7 count cm^{-2} sec^{-1}. The difference in flux measured at the two altitudes may be attributed principally to radiation of wavelengths longer than 6 Å. Unit optical thickness corresponded to 8 Å at 100 km and the spectrum was effectively cut off at about 10 Å. At 86.7 km, the wavelength for unit optical thickness was 4 Å. The combination of atmospheric opacity and reduced collimator transmission made the source undetectable against the background on scan 11, Fig. 1. We conclude that approximately one-third of the observed flux from the Scorpius source falls below 6 Å and two-thirds between 6 and 10 Å. If we attribute the x-ray emission to the black body radiation of a neutron star, the temperature of the Scorpius source, based on the present spectral evidence, would be in the neighborhood of 2 or 3 million degrees.

Three of the x-ray signals, labeled A, B, and I on the map of Fig. 1, appear to come from clearly isolated discrete objects. Signal I fits the position which we identified with the strong Scorpius source in 1963. Signal B was seen on three successive passes through the Cygnus region. The telemetry record of scan 4, when the source passed close to the center of the field of view, is reproduced in Fig. 2. The signal envelope is consistent with the expected angular response from a source of small angular width compared to the collimator aperture. Although Cygnus A, the brightest radio source in the sky, was within 6° of position B, there is no evidence of any x-ray contribution from it. Signal A was also discrete, and there is no outstanding optical or radio object at its position.

The portions of scans 5, 6, and 7 which cover the general region near the center of the galaxy reveal a complex of emission which can be best resolved as the sum of six "point" sources labeled C, D, E, F, G, and H. Table 1 lists the positions of the nine sources identified by the survey, the observed counting rates, and the fluxes computed for two assumed black body spectra. All of the listed sources were observed as signals clearly above background on each of two counters. Also included in Table 1 is the Crab Nebula. We have labeled the sources "XR" for x-ray, and numbered them within the various constellations according to brightness.

In the survey of 25 November, satisfactory data were obtained from three of the four x-ray counters. Despite the wide expanse of sky that was searched from Perseus to Puppis, the only source observed was the Crab Nebula. The flux was 2.7 count cm^{-2} sec^{-1} through ¼-mil Mylar and 1.6 count cm^{-2} sec^{-1} through ½-mil Mylar. This result contradicts the spectral observation of the Crab x-ray emission on 7 July 1964 (*3*). At that time the observations were made through windows of ¼-mil and 1-mil Mylar. No significant difference in counting rate was observed, which

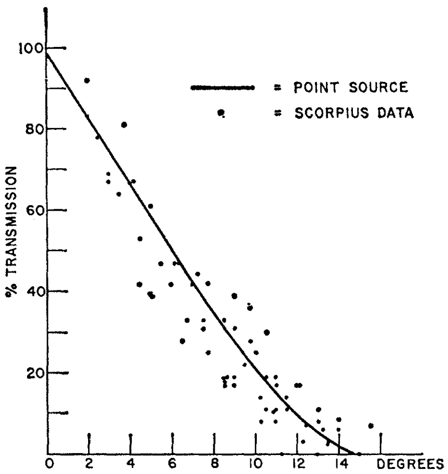

Fig. 3. Solid line is theoretical transmission curve of honeycomb collimator used in April 1963 Aerobee flight. From eight scans of the Scorpius region the peak position was located at $16^h\ 15^m$, $-15.2°$. The dots show the angular dependence of observed counting rates, with peak signal normalized to 100 percent transmission. Average displacement from transmission curve is $-0.2°$.

led us to conclude that the spectrum of Tau XR-1 (Taurus) was largely concentrated below 5 Å. We only comment here on the photometry problem (*4*). It has been necessary to treat these counters with NO_2 gas in order to desensitize any response to ultraviolet light. Mylar presents additional problems due to its water vapor permeability. The combination of curing treatment and water vapor can reduce the volume sensitivity and long wavelength response of the counter. We have referred (*3*) to evidence of such an effect, as indicated by the relative insensitivity of the counter with ¼-mil Mylar window compared to the counter with a 1-mil window. For the 25 November flight we introduced important new procedures to preserve the sensitivities of the counter tubes and have confidence that the indication of strong emission from the Crab at wavelengths longer than 5 Å is valid.

The surveys completed thus far cover about 70 percent of the celestial sphere. All of the x-ray sources observed lie rather close to the galactic plane and within 90° of the galactic center. This distribution resembles that of galactic novae and suggests that all of the x-ray sources thus far observed may be associated with supernova remnants in the galaxy. Taurus XR-1 was located by the lunar occultation observation of 7 July 1964, within 1 arc minute of the center of the Crab Nebula. Ophiuchus XR-1 fits the position of the 1604 Kepler supernova within the 1.5° accuracy of the observation.

There appear to be at least two types of x-ray "stars," those associated with radio and visible sources, such as Tau XR-1, Oph XR-1, and possibly Sgr XR-2 (Sagittarius), and those like Sco XR-1, Cyg XR-1, and Cyg XR-2, which are not identified with radio or optical sources at their positions. Although the occultation observation of Tau XR-1 showed that its diameter was about 1 light-year, little is known of the dimensions of the remaining x-ray stars, other than that they appear small compared to the aperture of the collimator. In the April 1963 observation of Sco XR-1 it was scanned eight times. We have re-examined those data in reference to the angular transmission of the collimator to see if a more precise limit on angular size can be deduced. The computed angular dependence of transmission was checked by direct measurement in the laboratory with both visible light and x-rays (solid line, Fig. 3). The distribution of observed counting rates plotted against angular displacements from the peak intensity is shown by the dots in Fig. 3. The displacement of the average of the measured pattern from the collimator transmission curve for a point source is $-0.2°$. We conclude that the true size of the Scorpius source is probably less than 0.2°.

We referred (*3*) to the association of the Scorpius source with the North Polar Spur observed by radio astronomers. It has been suggested (*5*) that the Spur is the nebular remains of a supernova explosion which occurred at about 30 parsecs (pc) from the sun, 50,000 to 100,000 years ago. Shklovsky (*6*) considered that the x-ray source may be similar in size to the Crab and that both were probably synchrotron radiators. If the Scorpius source were 1 light-year in diameter, as is the Crab, its angular size at 100 light-years would be about 0.6°. Since our observations indicate that Sco XR-1 is less than 0.2° in diameter, it must be smaller than Tau XR-1, if it is closer than 100 light-years. The opacity of interstellar gas increases very rapidly with increasing wavelength. At 100 light-years, however, it should be possible to observe a wavelength as long as 50 Å. Observations of Sco XR-1 in the range of 44 to 50 Å should confirm its relatively close proximity to the sun.

Neutron star models have recently been revised to conform to much faster neutrino cooling rates (*7*). As a result, the x-ray source temperature would fall below 10^7 degrees Kelvin in a matter of a few years. At 2 or 3 million degrees Kelvin however, cooling proceeds relatively slowly by electromagnetic radiation loss. A life of 50,000 years is consistent with the observed flux of Sco XR-1 if it is, in fact, closer than 100 light-years.

The nature of the x-ray production processes in Tau XR-1 is still very much subject to speculation. In discussing the spectral data of 7 July 1964 (*3*) we stressed that the spectrum appeared to be attenuated at long wavelengths more rapidly than synchrotron radiation with a spectral coefficient (γ) equal to -1.1. We now suspect that the spectral data of that flight were not valid. Furthermore, the spectral fluxes (*3*, Table 1) had been incorrectly calculated and the synchrotron flux for the ¼-mil Mylar window was in error by a factor of 10. The apparently poor fit of the synchrotron spectrum, as compared to a thermal spectrum, was, therefore, grossly exaggerated. The new

Table 1. X-ray sources. Flux is uncorrected for atmospheric absorption. It was measured with a ¼ mil Mylar window. Column *A* is the flux (10^{-8} erg cm^{-2} sec^{-1}) computed for a black body at 2×10^7 degrees Kelvin, 1.5 to 8 Å, and Column *B* is that for a black body at 5×10^6 degrees Kelvin, 1.5 to 8 Å.

1950 Epoch		Flux		
R.A.	Declination (deg)	Obs. (count cm^{-2} sec^{-1})	*A*	*B*
		*Tau XR-1**		
$05^h31.5^m$	22.0	2.7	5.5	1.1
		Sco XR-1†		
16^h15^m	−15.2	18.7	38	7.9
		Sco XR-2		
17^h8^m	−36.4	1.4	2.9	0.6
		Sco XR-3		
17^h23^m	−44.3	1.1	2.3	0.5
		Oph XR-1‡		
17^h32^m	−20.7	1.3	2.7	0.6
		Sgr XR-1§		
17^h55^m	−29.2	1.6	3.3	0.7
		Sgr XR-2‖		
18^h10^m	−17.1	1.5	3.0	0.6
		Ser XR-1		
18^h45^m	5.3	0.7	1.5	0.3
		Cyg XR-1		
19^h53^m	34.6	3.6	7.3	1.5
		Cyg XR-2		
21^h43^m	38.8	0.8	1.7	0.4

* Within 1′ of optical center of nebula. † Previous measurement (*2*) 12×10^{-8} erg cm^{-2} sec^{-1} computed as for column *A*. ‡ 1.1° from SN1604. § 2.3° from galactic center. ‖ 1.2° from M 17.

spectral evidence, based on the 25 November flight, can be fitted to a bremsstrahlung spectrum at about 10^7 degrees Kelvin, a black body spectrum at about 5×10^6 degrees Kelvin, and a synchrotron spectrum with $\gamma = -1.1$.

If Oph XR-1 is truly associated with supernova 1604, it may be meaningful to compare it with Tau XR-1, since both are presumably Type I supernovae. Recent distance estimates place the Crab at 1.5 kpc and the Kepler supernova at 9 kpc. Distance alone should make the Crab approximately 50 times as bright, but its x-ray flux is only twice as bright. The Crab, however, is 550 years older, and the weakness of its x-ray flux may be attributed to aging at the rate of about 5 percent per year.

In view of the theoretical predictions of x-ray emission from the region of the galactic center (*8, 9*), it is interesting to note that Sgr XR-1 is indeed close to the direction of the galactic center. We have located the x-ray source about 2.3° from Sgr A. The displacement appears to exceed our estimated positional uncertainty, but the difference is not so great as to rule out positively the possibility of a coincidence between the x-ray and radio source.

S. Bowyer, E. T. Byram
T. A. Chubb, H. Friedman
E. O. Hulburt Center for Space Research, U.S. Naval Research Laboratory, Washington, D.C.

References and Notes

1. R. Giacconi, H. Gursky, F. R. Paolini, B. B. Rossi, *Phys. Rev. Letters* **9**, 439 (1962); *ibid.* **11**, 530 (1963).
2. S. Bowyer, E. T. Byram, T. A. Chubb, H. Friedman, *Nature* **201**, 1307 (1964).
3. ———, *Science* **146**, 912 (1964). We call attention to an error in this paper. On line 4, the middle column, p. 913, change B to A, and on line 7 change A to B.
4. Complete discussion in preparation.
5. R. H. Brown, R. D. Davies, C. Hazzard, *Observatory* **80**, 191 (1960).
6. I. S. Shklovsky, *Astron. Tsirk. Akad. Nauk. SSSR*, No. 304 (1964).
7. A. G. W. Cameron, private communication.
8. R. J. Gould and G. R. Burbidge, *Astrophys. J.* **138**, 969 (1963).
9. S. Hayakawa and M. Matsuoka, *Progr. Theoret. Phys. Kyoto* **29**, 612 (1963).
10. Sponsored jointly by ONR and NSF.

23 December 1964

Ancient Oyster Shells on the Atlantic Continental Shelf

Abstract. *Shells of long-dead* Crassostrea virginica *are reported at 71 stations in depths of 14 to 82 meters. The depths exceed those of the estuaries where the species flourishes. Radiocarbon measurements indicate that the oysters were alive 8000 to 11,000 years ago. It is concluded that the oysters lived in lagoons or estuaries which became submerged when the sea level rose at the end of the latest glacial epoch.*

Many oyster shells were found in samples of bottom materials from the continental shelf between Cape Cod and Cape Hatteras. None of the samples contained living oysters. The oyster shells were identified as those of *Crassostrea virginica* (Gmelin) (*1*), the common edible species in estuaries along the Atlantic coast of the United States (*2*). The possibility that the shells were recently carried by currents from the mouths of present-day estuaries was not supported by the pattern of distribution. Nor was this possibility supported by the condition of the oyster shells, which, after they had dried, were observed to flake away easily as though the organic matrix in them had decomposed. Thus the depth, distribution, and character of the shells were suggestive of subfossils. Radiocarbon measurements of oysters from selected samples confirmed that the oysters were indeed ancient.

The oyster shells were found between Cape Cod and Cape Hatteras in dredge samples at 33 out of 113 stations of R/V *Delaware* (Cruise 60-7) in an investigation conducted by the U.S. Bureau of Commercial Fisheries during 1960 (*3*). A review of earlier data of the Bureau revealed the presence of the shells at one station of R/V *Albatross III* in 1955. During 1963, additional shells were found in large samples of bottom materials at 37 out of about 300 stations of R/V *Gosnold* between Cape Cod and Delaware Bay. These stations were occupied as part of a study of the geological history of the Atlantic continental shelf (*4*) being conducted by the Woods Hole Oceanographic Institution and the U.S. Geological Survey. The positions of all 71 stations where oyster shells were collected are given in Fig. 1. About 600 other bottom-sampling stations have been occupied by ships of the U.S. Bureau of Commercial Fisheries and the Woods Hole Oceanographic Institution east and northeast of Cape Cod, but no oyster shells were noted in that region. Samples south of Delaware Bay were largely restricted to the outer half of the continental shelf, thus accounting for the apparent restriction of oyster shells to that area (Fig. 1).

As shown in Fig. 2, the shells were found at water depths between 14 and 82 m, and there were some indications that they occurred in greater numbers at depths of about 38 m and 59 m. The water depths at all of the stations far exceed the depths at the intertidal or slightly subtidal positions of living oysters along the Atlantic coast. Compilation of the biological measurements showed that, on the average, the largest total numbers and weights of shells occurred at stations where the water depth was more than 30 m. Photographs of the bottom taken at the same time that the samples were collected aboard R/V *Gosnold* (*5*) showed the oyster shells resting on the surface of the bottom (Fig. 3) at only two stations. Evidently, most shells are buried in the sediment, where they were recovered from depths to 30 cm below the surface, the maximum depth of penetration of the large grab-sampler.

Studies of the geological history of the continental shelves of the world indicate that the shelves were exposed above sea level during the Pleistocene glacial stages (*6*). The latest such glaciation reached its climax about 18,000 years ago, after which the sea level gradually rose and allowed the shoreline to transgress the width of the continental shelf. Stages of transgression are recorded by drowned barrier bars and by terraces that commonly are four or five in number and occur throughout the world (*7, 8*) as well as within the area of Fig.

Table 1. Ages of *Crassostrea virginica* estimated by radiocarbon dating.

Station No.	North latitude	West longitude	Depth (m)	Bottom type	Age (yr)	Lab. No.*
(Living specimen)†	38°33′	76°13′	2		Modern	W–1399
Del. 7–1	36°09′	75°20′	33	Sand and shell	8,130±400	W–1402
Del. 26	38°49′	73°39′	55	Sand and shell	9,780±400	W–1403
Del. 45	40°43′	72°25′	37	Sand	9,920±400	W–1400
Del. 47	40°40′	71°59′	51	Sand and shell	10,850±500	W–1401

* U.S. Geological Survey, Radiocarbon Laboratory. † Collected by Jackson in 1924 (*12*).